RSC Advances

ROYAL SOCIETY OF CHEMISTRY

www.rsc.org/advances

RSC Advances

ARTICLE

Compressed Sodalite-like MgH_6 as a Potential High-temperature Superconductor

Received 00th January 20xx,
Accepted 00th January 20xx

DOI: 10.1039/x0xx00000x

www.rsc.org/

Xiaolei Feng,[a] Jurong Zhang,[a] Guoying Gao,[b] Hanyu Liu,*[c,d] and Hui Wang*[a]

Recently, an experimental work reported a very high T_c of ~190K in hydrogen sulphide (H_2S) at 200 GPa. The search of new superconductors with high superconducting critical temperatures in hydrogen-dominated materials has attracted significant attention. Here we predict a candidate phase of MgH_6 with a sodalite-like framework in conjunction with first-principles electronic structure calculations. The calculated formation enthalpy suggests that it is thermodynamically stable above 263 GPa relative to MgH_2 and solid hydrogen (H_2). Moreover, the absence of imaginary frequency in phonon calculations implies that this MgH_6 structure is dynamically stable. Furthermore, our electron-phonon coupling calculation based on BCS theory indicates that this MgH_6 phase is a conventional superconductor with a high superconducting critical temperature of ~260 K under high pressure, which is even higher than that of the recently reported compressed H_2S. The present results offer insights in understanding and designing new high-temperature superconductors.

Introduction

The search of new superconductors with high critical temperatures (T_c) has attracted great intention due to the discovery of superconductivity of mercury in 1911.[1] For conventional Bardeen-Cooper-Schrieffer (BCS) superconductors, MgB_2 was found to possess a T_c of 39 K.[2] However, there are no other conventional superconducting compounds to be found to have a higher T_c than that of MgB_2. For other unconventional superconducting compounds, the last several decades have witnessed an exciting revolution in searching high-temperature superconductivity materials, such as cuprates and iron-base superconductivity materials, but their superconducting mechanism cannot be explained by Bardeen-Cooper-Schrieffer (BCS) theory and still raises a source of debate.[3-5] Ashcroft suggested the metallic phase of solid hydrogen should possess high-temperature conductivity.[6] Until now, solid hydrogen has not been found to become metallic until up to 360 GPa in laboratory.[7] It is noted that a recent theoretical work proposed that H_2S may become a good superconductor above 100 GPa.[8] Soon after that a high-pressure electrical measurement well proved that the compressed H_2S can become a superconductor with a very high T_c of ~190K at 200 GPa.[9] On the other hand, another theoretical work also suggest that $(H_2S)_2H_2$ is a good superconductor with T_c of 191-204K at 200 GPa.[10] There have also been many theoretical efforts in studying the superconducting mechanism of H_2S and investigating whether the compressed H_2S is stable and dissociate into other Sulfur hydrides.[11-18] At present, the superconducting mechanism of compressed H_2S is not quite clear and remains elusive. Therefore, investigates of other relevant hydrides are important as well as helpful in shedding light on the intricate superconducting mechanism and providing ideas for new potential high-temperature superconductor design.

Recently, CaH_6 has been predicted to have a good superconductivity of 235 K at 150 GPa.[19] This structure consists of a sodalite-like hydrogen cage filled with interstitial Calcium (Ca) atoms. Due to the similarity between Mg and Ca, Mg may also adopt a sodalite-like structure with hydrogen atoms. Therefore, it is interesting to explore the stability of sodalite MgH_6 structure and its potential superconducting behaviors. Moreover, another recent theoretical work also suggests that YH_6 adopts this sodalite structure with a T_c of 251-264 K at 120 GPa.[20] A recent study based on evolutionary structure searches suggested that MgH_4 can be stable with respect to decomposition into MgH_2 and H_2 near 100 GPa, and it remains the most stable stoichiometry until at least 200 GPa.[21]

In this work, we study the stability of MgH_6 relative to MgH_2 and H_2 on the basis of first-principle density functional theory. The calculations indicate that the MgH_6 is dynamically stable and thermodynamically stable above 263 GPa. Further electron-phonon coupling calculations imply that this MgH_6 phase possesses very good superconductivity with a high superconducting critical temperature of ~260K above 300 GPa. Our current results also show that the charge transfer

[a] State Key Laboratory of Superhard Materials, Jilin University, Changchun 130012, China
[b] Material Science and Nanoengineering, Rice University, Houston, 77005, USA
[c] Geophysical Laboratory, Carnegie Institution of Washington, 5251 Broad Branch, Road N.W. Washington D.C. 20015, USA
[d] Department of Physics and Engineering Physics, University of Saskatchewan, Saskatoon, Saskatchewan S7N 5E2, Canada.
* Address correspondence to: haliu@carnegiescience.edu or huiwang@jlu.edu.cn
Electronic Supplementary Information (ESI) available: [details of any supplementary information available should be included here]. See DOI: 10.1039/x0xx00000x

between Mg and H atoms and H-H interactions are responsible for this good superconductivity. We find that the calculated T_c of this MgH_6 phase increases up to above 300 GPa.

Results

Inspired by our previous work[19] predicting high superconductivity of CaH_6 where Hydrogen atoms adopt a sodalite-like framework that is responsible for high superconductivity, we have replaced Ca atoms by Mg atoms in this sodalite-like structure. This structure was optimized with fully relaxing the atoms and lattice parameters within first-principles electronic structure framework, which produces a body centered cubic (bcc) crystal structure and space group of *Im*-3*m* with 14 atoms per unit cell, in agreement with our previous work.[19] To investigate the thermodynamically stability, we have calculated the formation enthalpy relative to MgH_2 and H_2 (Fig. 1), where previously predicted *P*6$_3$/*mmc* Ni_2In-type structure[21] was used for MgH_2 and *C*2/*c* and *Cmca*-12 structure[22] were used for solid hydrogen. Interestingly, this MgH_6 is stable above 322 GPa which is higher than 150 GPa in CaH_6. This is not unreasonable since the light elements adopt low-pressure structures for heavy elements.[23] On the other hand, MgH_6 is a hydrogen-dominated material where hydrogen is the lightest element and has a large zero-point (ZP) energy that may revise the stability range at high pressures. To account for the ZP effects, we estimated the ZP energies for MgH_6, MgH_2 and H_2, using a harmonic method.[24, 25] As shown in the inset of Fig. 1, the inclusion of the ZP energies does shift down the stability of this MgH_6 phase from 322 GPa to 263 GPa. This indicates that the ZP effect is further helpful to stabilize this newly predicted MgH_6 structure.

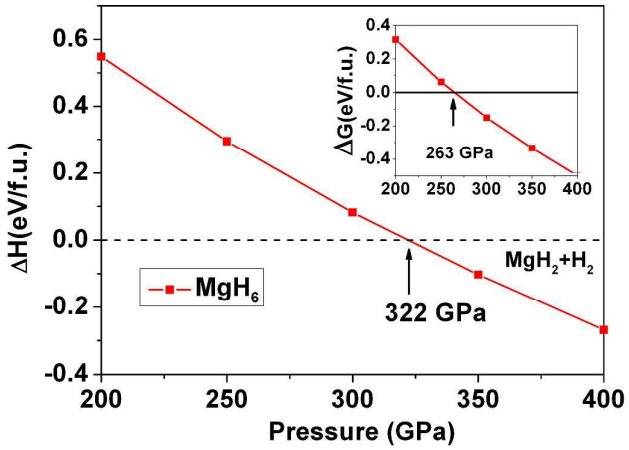

Fig. 1 The calculated formation enthalpy of MgH_6 relative to MgH_2 and H_2. The inset shows the formation energy of MgH_6 with considering zero-point energy effects.

The sodalite-like MgH_6 structure is shown in Fig. 2a, each hydrogen atom has four neighbor hydrogen atoms with distance of 1.1Å at 300 GPa. The H and Mg atom situate 2d position (0, 0.25, 0.5) and 2a position (0, 0, 0), respectively. The distance between hydrogen atoms is similar to the distance in atomic phases of solid hydrogen (e.g. 1.0Å in Cs-IV structure of solid hydrogen at 500 GPa). It is noted that one previous theoretical work suggests that the atomic phases of solid hydrogen possess good superconductivity under high pressure.[26] The similar bonding behaviors suggest that MgH_6 may be a good superconductor as well. To further gain insight into the interactions between hydrogen atoms, we have calculated the electron localization function (ELF).[27] The topological analysis of ELF is commonly used to determine the degree of electron localization and subsequently, the tendency to form two electron covalent bonds in molecules and solids. Represented in a convenient scale, ELF=1 corresponds to perfect localization and at the low limit ELF=0.5 reflects the behavior of a homogeneous electron gas. The contour plot of the ELF for this MgH_6 structures is shown in Fig. 2b. The strong interaction between hydrogen atoms can be clearly seen. Moreover, we have carried out Bader calculations on this MgH_6 structure using the quantum theory of atoms-in-molecules (AIM).[28] In the AIM theory, an atom within a solid is defined through the "zero-flux" condition of the electron density gradient. The results suggest that each Mg atom donates 1.63 electrons and each hydrogen atom attractes 0.27 electrons. This charge transfer may help enhance the interactions between hydrogen atoms.

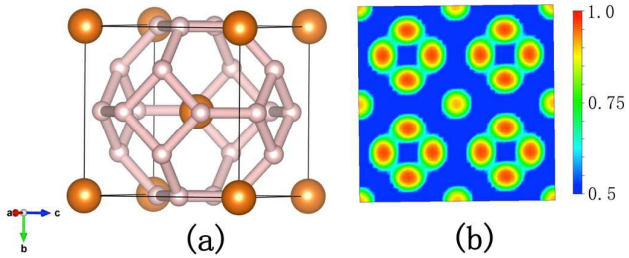

Fig. 2 (a) The structure of MgH_6. The small and big spheres represent H and Mg stoms, respectively. (b) The 2-dimemsional electron localization function in {100} plane is shown with a 2×2 supercell at 300 GPa.

Discussion

To investigate the electronic states, band structure for this MgH_6 structures was calculated as shown in Fig. 3. The results clearly show that this phase is a metallic phase, which is in good agreement with the previous results.[19] The projected density of states in Fig. 3 show that the H_s orbit is also important for the contribution of this metallization. There are two bands crossing the Fermi level (Fig. 3). This results in a high electronic density states at the Fermi energy (Fig. 3). Moreover, there are two parallel bands along the H-N-P direction, which is helpful to form Fermi nesting that can induce strong electron-phonon coupling. The band dispersion along P-Γ-N direction is parabolic-like and close to the Fermi level. One band crossing along the N-P direction with steep slopes indicates the existence of mobile electrons along these symmetry directions. The co-existence of electrons with large effect masses (flat band around Γ and P) and itinerant

electrons with high mobility (steep bands in H-N, N-P and P-Γ) suggested the possibility of high superconductivity.

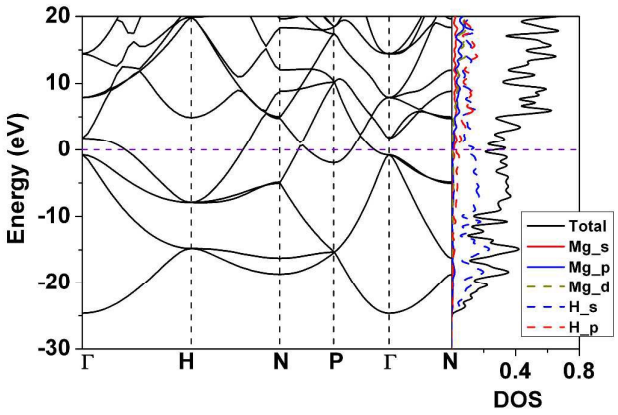

Fig. 3 The calculated band structure and density of states of MgH_6 structure at 300 GPa.

As mentioned above, the electronic band structure of MgH_6 shows the existence of sharp and flat bands crossing the Fermi energy level, indicative of its possible superconductivity. In order to investigate the superconductivity of MgH_6, phonon band structures, phonon density of states (PHDOS) and Eliashberg spectral function $\alpha^2F(w)$ for MgH_6 were carried out. As shown in Fig. 4. There is no imaginary frequency to be found in the whole Brillouin zone (BZ), confirming that it is a dynamically stable structure.

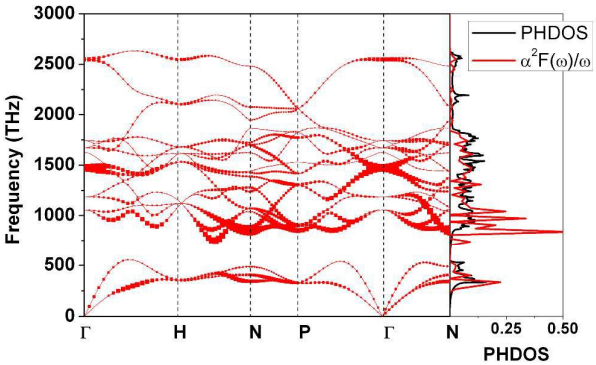

Fig. 4 The calculated phonon band structure, phonon density of states and Eliashberg spectral function of MgH_6 at 300 GPa.

Circles with a radius proportional to the electron-phonon coupling strength were also plotted in Fig. 4, to illustrate the contributions associated with different phonon modes. One can observe that nearly all phonon modes contribute to the whole Brillouin zone, reflecting a three-dimensional superconducting nature of the MgH_6 structure. Moreover, the superconductivity in MgH_6 is associated with the Kohn anomalies observed in the phonon dispersion (Fig. 4). At 300 GPa (Fig. 4b), the electron-phonon coupling parameter (λ) for the MgH_6 structure is 3.29 with an average phonon frequency ln(ω) of 1450 K. Using the Allen Dynes equation,[29] which is an extension of the McMillan theory,[30] with a nominal Coulomb pseudopotential parameter (μ*) of 0.12 the estimated superconducting critical temperature T_c is 263 K.

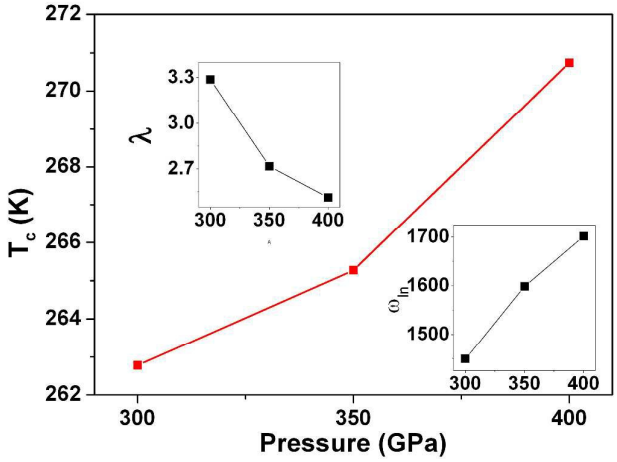

Fig. 5 Superconducting temperature (T_c) vs. pressure. The coupling parameters, the average phonon frequencies ω_{ln} and superconducting temperatures of MgH_6 as a function of pressure.

We have also studied the T_c of MgH_6 as a function of pressure. As shown in Fig. 5, the T_c increases in the pressure range of 300 to 400 GPa. Furthermore, it is found that the calculated λ decreases with increasing pressure, but the average frequency increases as expected. The competing between the λ and the average frequency results in the increased T_c with pressure. The origin of the superconductivity could be traced back by a comparison of the calculated Eliashberg spectral fuction ($\alpha^2F(\omega)$) and PHDOS. As shown in Fig. 4b, 15% of the electron phonon coupling is contributed to the low-frequency vibrations in the region from 0 to 600 cm^{-1}, which are mostly from the vibrations of Mg atoms. The remained 85% derives from high-frequency vibrations from 600 to 2600 cm^{-1} which are predominately H-H stretching and bending modes. The superconducting critical temperature of 263 K at 300 GPa is higher than 39K[2] in MgB_2 and even 190K[9] in recently measured solid H_2S.

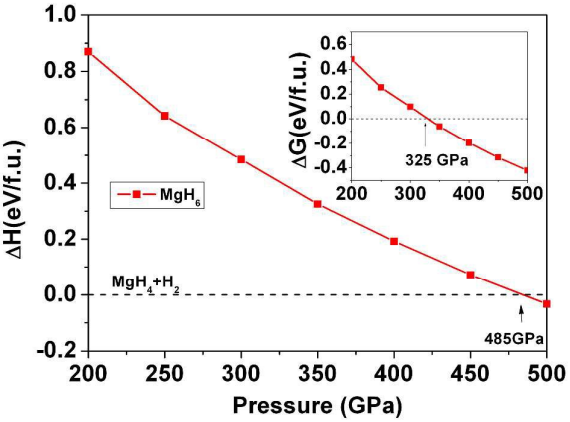

Fig. 6 The calculated formation enthalpy of MgH_6 relative to MgH_2 and H_2. The inset shows the formation energy of MgH_6 with considering zero-point energy effects.

Finally, we should point out that our calculated phase transition pressure (263 GPa) of MgH_6 is higher than that (~100

GPa) of MgH_4,[21] which means that MgH_4 is more thermodynamically stable than MgH_6 at low pressures. Furthermore, we have carried out the calculations on formation enthalpy of MgH_6 relative to MgH_4 and H_2 as shown in Fig. 6. It shows that MgH_6 actually thermodynamically stable relative to MgH_4 and H_2 above 325 GPa with considering ZP effects. However, it is noteworthy that MgH_6 is thermodynamically stable above 263 GPa relative to MgH_2 and H_2. Moreover, our phonon calculation confirms that is still a dynamically stable structure. These results suggest MgH_6 may be synthesized above 263 GPa with starting materials of MgH_2 and H_2. We also envisage that our predicted MgH_6 structure could possess a very high superconducting temperature. This work will benefit the study of superconducting mechanism for conventional BCS superconductors.

Conclusions

In summary, we have proposed a sodalite-like MgH_6 structure within first-principles electronic structure framework. This newly predicted MgH_6 structure was found to be thermodynamically stable above 263 GPa on the basis of the formation enthalpy calculations relative to MgH_2 and H_2. The phonon calculations suggest that this MgH_6 structure is dynamically stable due to the absence of imaginary frequency in the whole BZ. Furthermore, our electron-phonon coupling calculations reveal that MgH_6 is a good BCS superconductor with a high superconducting critical temperature of ~260 K above 300 GPa. The electron-phonon calculations also suggest that the three-dimensional superconducting nature in this newly predicted MgH_6 structure. The calculated T_c of MgH_6 was found to increase at a pressure range from 300 to 400 GPa with the decrease of the calculated λ and the increase of average frequency under compression. Our finding will stimulate future experimental study on synthesis of Magnesium hydrides and explore its high-Tc superconductivity under high pressure.

Computational details

Structural optimizations and enthalpy calculations were carried out with the Vienna *ab initio* simulation (VASP)[31-33] program and projector-augmented planewave (PAW)[34] potentials employing the Perdew–Burke–Ernzerhof (PBE)[35] functional. The valence configurations for the H and Mg potentials are $1s^1$ and $2s^2 2p^6 3s^2$, respectively. A plane wave basis set with an energy cutoff of 800 eV was used. Dense k-point meshes were employed to sample the first Brillouin zone (BZ) to ensure the energies are converged within 5 meV/atom. The elements of the interatomic force constant (IFC) and electron-phonon coupling matrices were computed using the linear response method with a 4×4×4 q-point mesh and 24×24×24 k-point mesh for the first Brillouin zone integrations.[36] A plane wave basis set with an energy cutoff of 80 Ry was used.

Acknowledgements

H. W. appreciatively acknowledges the financial support by Natural Science Foundation of China under Grants No. 11474128 and the 2013 Program for New Century Excellent Talents in University. Part of the calculations has been performed by the use of computing resources provided by WestGrid and Compute Canada. Hanyu Liu acknowledges the support from the University of Saskatchewan research computing group and the use of the HPC resources (Plato machine).

References

1 D. Van Delft and P. Kes, *Physics Today*, 2010, **63**, 38-43.
2 J. Nagamatsu, N. Nakagawa, T. Muranaka, Y. Zenitani and J. Akimitsu, *Nature*, 2001, **410**, 63-64.
3 G. Sun, K. Wong, B. Xu, Y. Xin and D. Lu, *Phys. Lett. A*, 1994, **192**, 122-124.
4 Y. Kamihara, H. Hiramatsu, M. Hirano, R. Kawamura, H. Yanagi, T. Kamiya and H. Hosono, *J. Am. Chem. Soc.*, 2006, **128**, 10012-10013.
5 Y. Kamihara, T. Watanabe, M. Hirano and H. Hosono, *J. Am. Chem. Soc.*, 2008, **130**, 3296-3297.
6 N. W. Ashcroft, *Phys. Rev. Lett*, 1968, **21**, 1748.
7 C. S. Zha, Z. Liu and R. J. Hemley, *Phys. Rev. Lett.*, 2012, **108**, 146402.
8 Y. Li, J. Hao, H. Liu, Y. Li and Y. Ma, *J. Chem. Phys*, 2014, **140**, 174712.
9 A. Drozdov, M. Eremets and I. Troyan, *arXiv preprint arXiv:1412.0460*, 2014.
10 D. Duan, Y. Liu, F. Tian, D. Li, X. Huang, Z. Zhao, H. Yu, B. Liu, W. Tian and T. Cui, *Sci. Rep.*, 2014, **4**, 6968.
11 J. Hirsch and F. Marsiglio, *Physica C: Superconductivity and its Applications*, 2015, **511**, 45-49.
12 D. Papaconstantopoulos, B. Klein, M. Mehl and W. Pickett, *Phys. Rev. B*, 2015, **91**, 184511.
13 D. Duan, X. Huang, F. Tian, D. Li, H. Yu, Y. Liu, Y. Ma, B. Liu and T. Cui, *Phys. Rev. B*, 2015, **91**, 180502.
14 D. Papaconstantopoulos, B. Klein, M. Mehl and W. Pickett, *Phys. Rev. B*, 2015, **91**, 184511.
15 V. V. Struzhkin, *Physica C: Superconductivity and its Applications*, 2015, **514**, 77-85.
16 N. Bernstein, C. S. Hellberg, M. Johannes, I. Mazin and M. Mehl, *Phys. Rev. B*, 2015, **91**, 060511.
17 I. Errea, M. Calandra, C. J. Pickard, J. Nelson, R. J. Needs, Y. Li, H. Liu, Y. Zhang, Y. Ma and F. Mauri, *Phys. Rev. Lett.*, 2015, **114**, 157004.
18 A. P. Durajski, R. Szcze and Y. Li, *Physica C: Superconductivity and its Applications*, 2015, **515**, 1-6.
19 H. Wang, S. T. John, K. Tanaka, T. Iitaka and Y. Ma, *Proc. Nati. Acad. Sci.*, 2012, **109**, 6463-6466.
20 Y. Li, J. Hao, H. Liu, S. T. John, Y. Wang and Y. Ma, *Sci. Rep.*, 2015, **5**, 9948.
21 D. C. Lonie, J. Hooper, B. Altintas and E. Zurek, *Phys. Rev. B*, 2013, **87**, 054107.
22 C. J. Pickard and R. J. Needs, *Nature. Phys.*, 2007, **3**, 473-476.

23 M. I. McMahon and R. J. Nelmes, *Chem. Soc. Rev.*, 2006, **35**, 943-963.
24 H. Liu, H. Wang and Y. Ma, *J. Phys. Chem. C*, 2012, **116**, 9221-9226.
25 H. Liu, L. Zhu, W. Cui and Y. Ma, *J. Chem. Phys*, 2012, **137**, 074501.
26 J. M. McMahon and D. M. Ceperley, *Phys. Rev. B*, 2011, **84**, 144515.
27 A. D. Becke and K. E. Edgecombe, *J. Chem. Phys*, 1990, **92**, 5397-5403.
28 R. F. Bader, *Acc. Chem. Res.*, 1985, **18**, 9-15.
29 R. D. P. B. Allen, *Phy. Rev. B*, 1975, **12**, 905.
30 R. Dynes, *Solid State Commun.*, 1972, **10**, 615.
31 G. Kresse and J. Furthmüller, *Phys. Rev. B*, 1996, **54**, 11169.
32 G. Kresse and J. Hafner, *Phys. Rev. B*, 1994, **49**, 14251.
33 G. Kresse and J. Hafner, *Phys. Rev. B*, 1993, **47**, 558.
34 P. E. Blochl, *Phys. Rev. B*, 1994, **50**, 17953.
35 J. P. Perdew, K. Burke and M. Ernzerhof, *Phys. Rev. Lett.*, 1996, **77**, 3865-3868.
36 P. Giannozzi, S. Baroni, N. Bonini, M. Calandra, R. Car, C. Cavazzoni and D. Ceresoli, *J. Phys. Condens. Matter*, 2009, **21**, 395502.